

Distributions and Structure of the Solar Wind during Solar Cycles 23 and 24

Somaïla Koala*, Wendkouni Paulin Bere, Yacouba Sawadogo, Issamaïl Ki, Jean Louis Zerbo

Laboratoire de Matériaux, d'Héliophysique et Environnement (La.M.H.E), Université Nazi BONI, Bobo-Dioulasso, Burkina Faso
Email: *ismaelkoala@yahoo.com

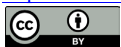
How to cite this paper: Koala, S., Bere, W.P., Sawadogo, Y., Ki, I. and Zerbo, J.L. (2023) Distributions and Structure of the Solar Wind during Solar Cycles 23 and 24. *International Journal of Geosciences*, 14, 813-826.
<https://doi.org/10.4236/ijg.2023.149043>

Received: July 25, 2023

Accepted: September 3, 2023

Published: September 6, 2023

Copyright © 2023 by author(s) and Scientific Research Publishing Inc. This work is licensed under the Creative Commons Attribution International License (CC BY 4.0).
<http://creativecommons.org/licenses/by/4.0/>



Open Access

Abstract

To observe the level of interaction between the solar wind and the geomagnetic activity, we analyzed the distribution of the solar wind speeds according to the different classes of geomagnetic activity and the different phases of solar activity. We found that, the magnetic quiet activity record 80% of the solar wind speeds $V < 450$ km/s. The recurrent activity has observed 88% of solar wind speeds $V > 450$ km/s. The shock activity observes 82% of the solar wind speeds $V > 450$ km/s. About 70% of the solar wind speeds $V > 450$ km/s, are observed in the corotating activity class. The cloud shock activity and fluctuating activity classes observed respectively 37% and 55% of the wind speeds $V > 450$ km/s. Furthermore, slow solar winds are mainly observed at the minimum phase of each solar cycle; but exceptionally the solar maximum phase of solar cycle 24, records a significant rate of slow solar wind. Shock winds are mainly observed around the solar maximum and recurrent winds are mainly observed at the descending phase of the solar cycle. Corotating stable winds and moderate shock winds dominate respectively at the descending phase and at the maximum phase.

Keywords

Solar Wind, Solar Activity, Geomagnetic Activity, Solar Cycle

1. Introduction

The solar wind is a stream of plasma particles consisting mainly of ions and electrons that are ejected from the upper atmosphere of the Sun. Its structure varies in latitude with the cycle of solar activity. At the sunspot minimum, the solar wind is strongly structured by solar latitude [1]. The fast and tenuous solar wind comes from the polar coronal holes associated with the “open” magnetic flux [2]

[3] [4] and [5] and the slower and denser solar wind comes from equatorial flute belts associated with closed magnetic loops [6]. The solar wind spreads almost radially throughout the heliosphere, meaning that the large-scale structure of the solar wind at 1 AU is determined primarily by conditions in the upper corona [7]. Transient structures resulting from coronal mass ejections [8] propagate through “ambient” solar structures. While interplanetary CMEs (ICMEs) are responsible for the most severe space weather [9] [10], correctly predicting the structure of the ambient solar wind is important for space weather because the ambient solar wind, in particular fluxes from interaction regions (SIR), can be geoeffective per se [10] [11]. Then the ambient solar wind can modulate both the arrival time and the properties of ICMEs in near-Earth space [12] [13] [14]. Moreover, the ambient solar-wind structure is important for the magnetic connectivity between the Sun and the Earth, which determines the transport of solar energetic particles [15] [16]. The study of the structure and morphology of the solar plasma provides information on the dynamics of our Star. In this work, we will quantify the relationships between the solar wind, solar and geomagnetic activity according to the different classes established by [4] [17] and recently improved by [2]: quiet activity, recurrent activity, shock activity, magnetic cloud activity, corotating activity and fluctuating activity. We used the pixel diagram method for geomagnetic activity [2] [4] [17] and solar wind activity [2]. Our work is structured as follows: in Section 2, we presented the data and methodology, followed by the results and discussion in Section 3, and in Section 4, a summary of our results.

2. Data and Methodology

In this work we used the daily averages of the solar wind speed and the annual sunspots number available on the site <http://omniweb.gsfc.nasa.gov/ow.html>, in order to have a view overview of the structure and morphology of the solar plasma, according to the different classes of solar and geomagnetic activity. The determination of the different classes of solar and geomagnetic activity is done on the basis of Pixel diagrams using the criteria of [2]. Thanks to the close solar wind-Aa index correlation established by [18] and the classification of [2], the different classes of solar activity are organized as follows:

1) Quiet activity: day with $Aa < 20$ nT. Refers to slow solar wind from the solar heliosheet and very quiet days without thunderstorm activity defined by $V < 350$ km/s (white pixels in the diagram) and quiet days characterized by 350 km/s $< V < 450$ km/s (blue color in the pixel diagram). An example of a pixel diagram is shown in **Figure 1(a)** and **Figure 1(b)**.

2) Recurrent activity: $Aa \geq 40$ nT over at least one solar rotation (effects of fast winds). The class of recurrent winds, is formed by recurrent strong solar winds originating from coronal holes and extended over several solar rotations and characterized by $V \geq 550$ km/s ((orange, red and olive-red colors in the pixel diagram (**Figure 1(a)** and **Figure 1(b)**)).

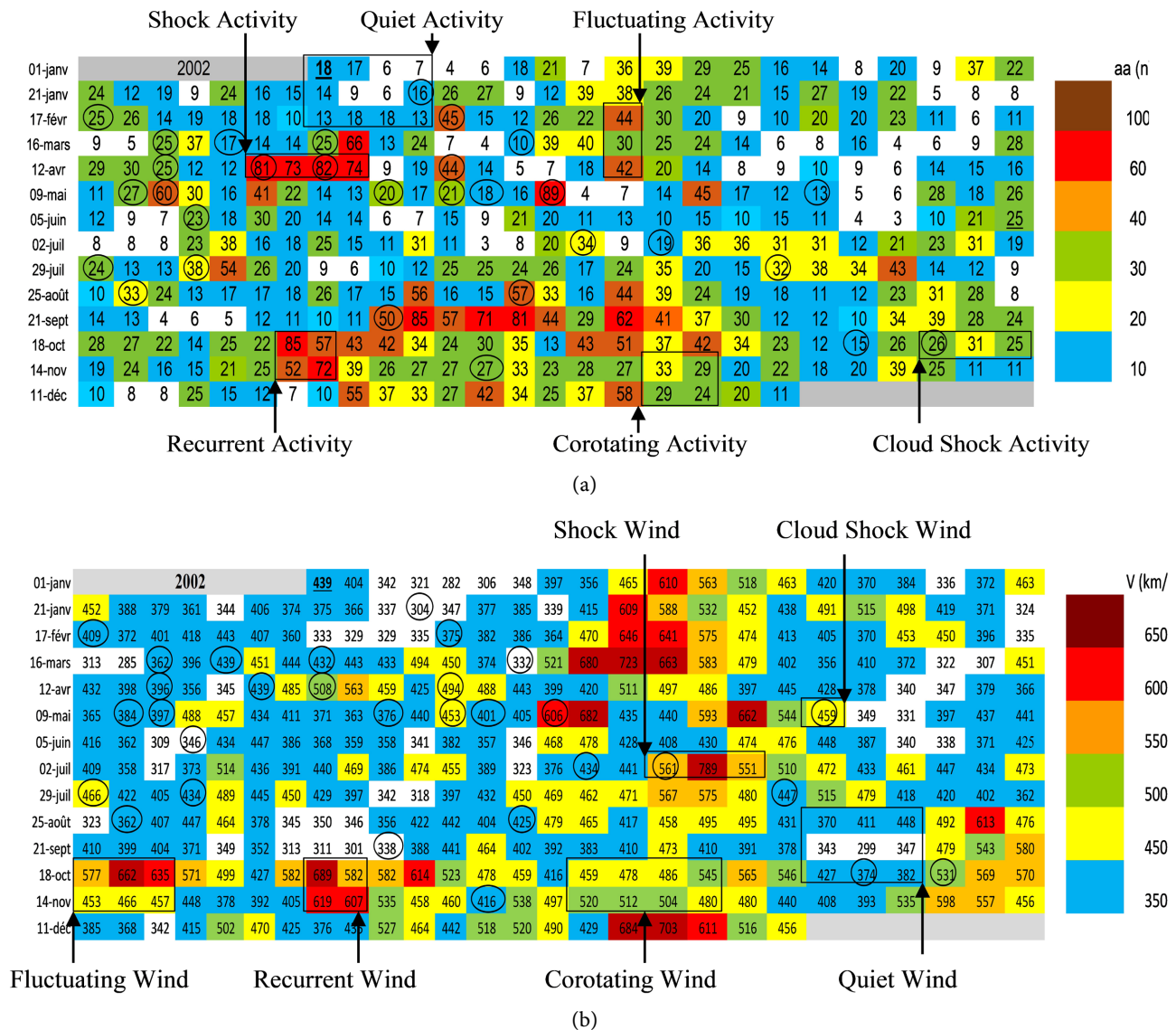


Figure 1. Pixel of the Aa index (a) and the speed (b) of the year 2002.

3) Shock activity: date of sudden onset of magnetic storms with Aa ≥ 40 nT over a period of 3 days at most (shock waves). The shock wind class is made up of days under CME events (circle on pixel diagram) and characterized by V ≥ 550 km/s with a duration of one, two or three days.

4) Corotating activity: the geomagnetic index is such that 20 nT ≤ Aa < 40 nT. This class is defined as the manifestation of solar winds, corotating stables and having moderate magnetic effects in the vicinity of the Earth’s environment; under these conditions the wind speeds are between 450 km/s and 550 km/s corresponding to the yellow and green colors on the wind speed pixel diagram. We identify this class by the recurrence zones without SSC (yellow and green colors in Figure 1(a) and Figure 1(b));

5) Magnetic cloud activity: the days selected are the SSC dates whose effect lasts one to three days. And the corresponding Aa range from 20 nT to 40 nT.

This activity groups together shock events causing a suitable change in the level of geomagnetic activity; corresponding to the speeds includes between 450 km/s and 550 km/s (yellow and green colors in **Figure 1(a)** and **Figure 1(b)**);

6) The fluctuating wind class: is made up of unidentified days in the two previous well-organized classes ($V \geq 450$ km/s). This is the class of transient and fluctuating events that are not taken into account in the previous classes. We evaluate its global energy level by subtracting from the fluctuating activity [4] the energy levels of the co-rotation class and magnetic clouds.

The start dates of sudden storms (Sudden Storm Commencement: SSC) are available on the site <https://isgi.unistra.fr>. For the distribution of speeds by interval, we have selected the dates and the daily values of the Aa index for each class of geomagnetic activity with the corresponding wind speeds. Then through the pixel diagram of the solar wind, we calculated the percentages of solar activity classes for each year and according to the different phases of solar activity, during the two solar cycles (solar cycles 23 and 24). **Figure 1** presents an example of the pixel diagram of the Aa index and the solar wind.

3. Results and Discussions

Figure 2 presents the solar wind distributions (a) and (b) and the percentage

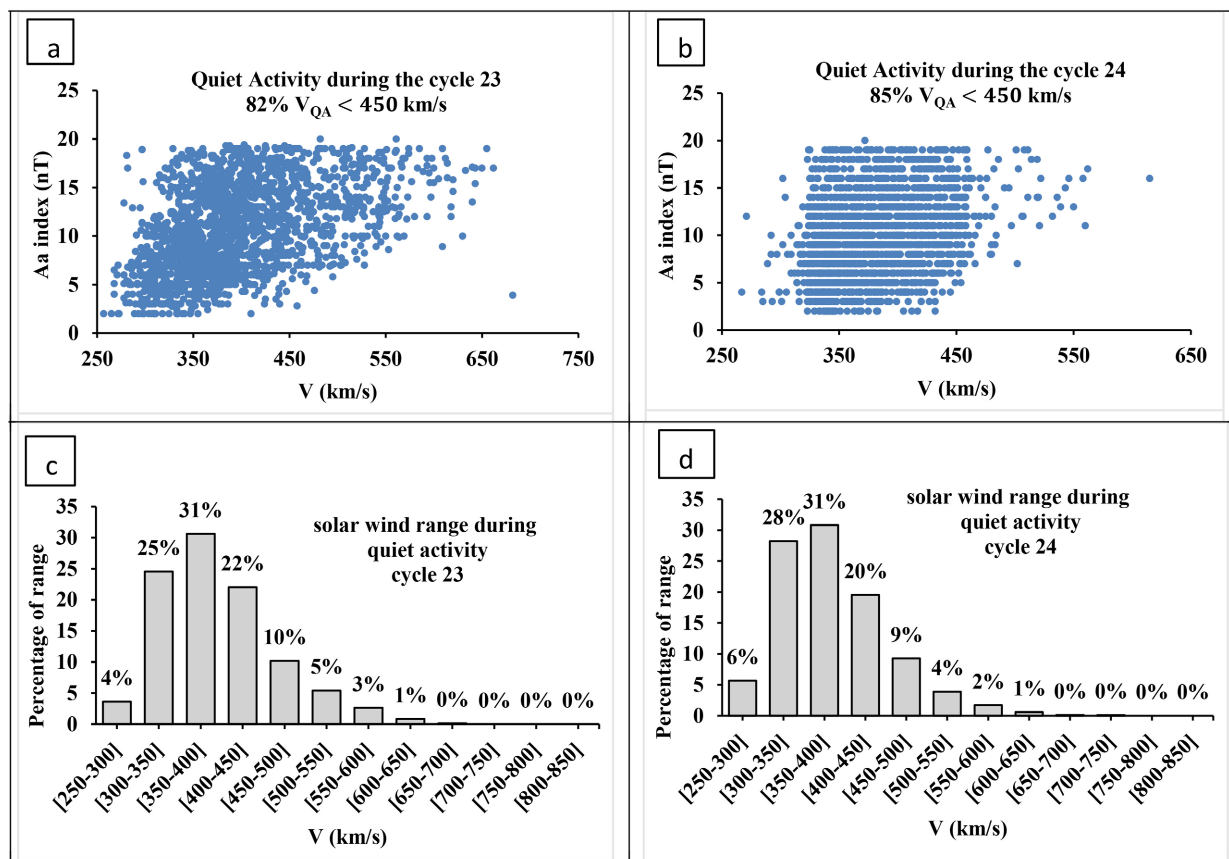


Figure 2. Solar wind distribution (a) and (b) and percentage distribution of solar wind speeds (c) and (d) in the quiet activity class during solar cycles 23 and 24.

distributions of solar wind speeds (c) and (d) in the quiet activity class during solar cycles 23 and 24. In this figure, we observed that 82% and 85% of the solar wind speeds respectively during solar cycles 23 and 24 blowing during quiet activity are less than 450 km/s. In addition, statistical analysis shows that during quiet activity 71% of solar wind speeds are of the order of 391 ± 68 km/s.

Figure 3 presents the solar wind distributions (a) and (b) and the percentage distribution of solar wind speeds (c) and (d) in the recurrent activity class during solar cycles 23 and 24. This figure shows that 90% and 86% of the solar wind speeds respectively during solar cycles 23 and 24, during the recurrent activity are greater than 450 km/s. In addition, 65% of solar wind speeds are of the order of 575 ± 100 km/s.

Figure 4 presents the solar wind distributions (a) and (b) and percentage distribution of solar wind speeds (c) and (d) in the shock activity class during solar cycles 23 and 24. In this figure, we recorded that 78% and 86% of the solar wind speeds respectively during solar cycles 23 and 24, are greater than 450 km/s. We also observe that 69% of the solar wind speeds are of the order of 548 ± 110 km/s during the two solar cycles during the shock activity.

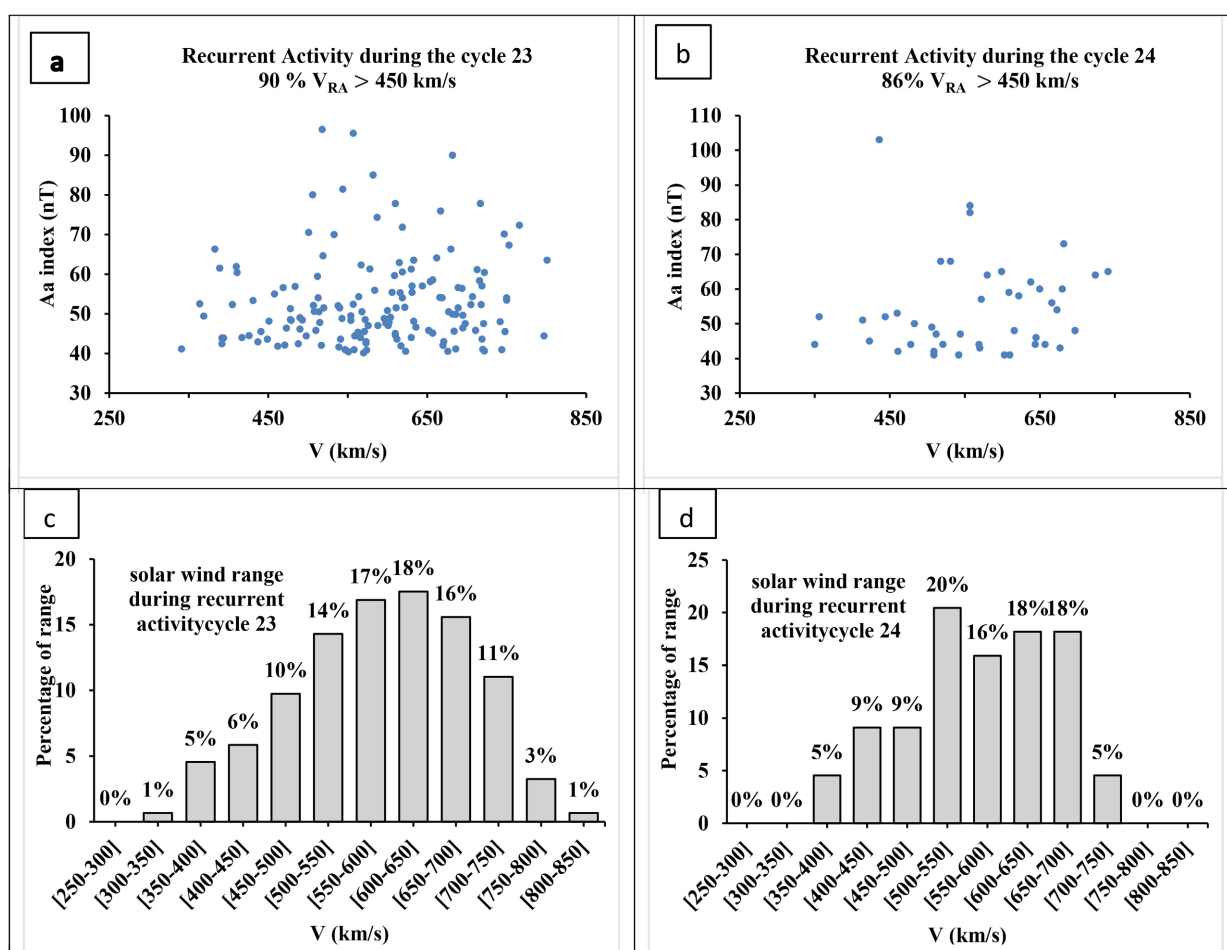


Figure 3. Distribution of solar wind (a) and (b) and percentage distribution of solar wind speeds (c) and (d) in the recurrent activity class during solar cycles 23 and 24.

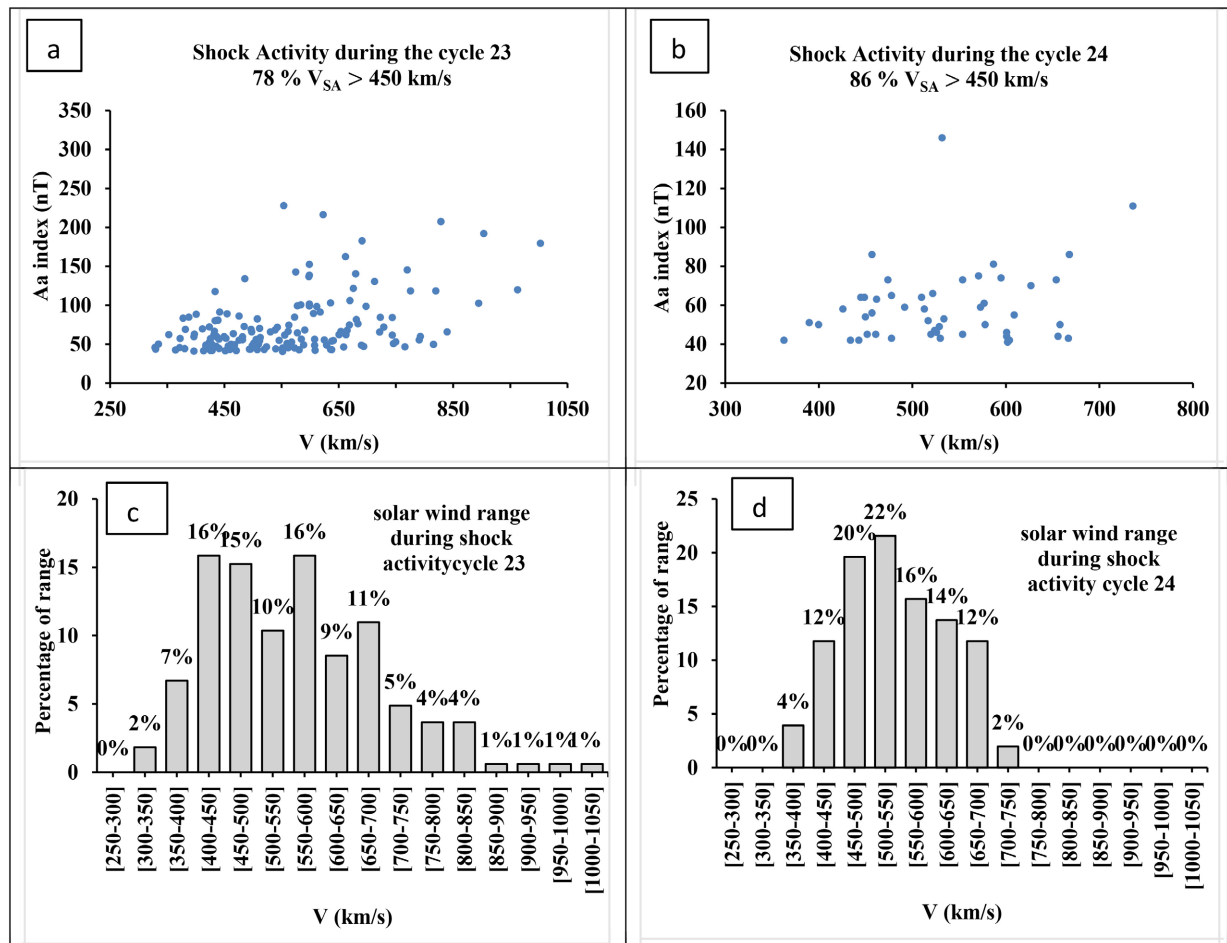


Figure 4. Solar wind distribution (a) and (b) and percentage distribution of solar wind speeds (c) and (d) in shock activity class during solar cycles 23 and 24.

Figure 5 presents the solar wind distributions (a) and (b) and the percentage distribution of solar wind speeds (c) and (d) in the class of corotating activity during solar cycles 23 and 24. This figure shows that 69% and 71% of the solar wind speeds respectively during solar cycle 23 and 24 are above 450 km/s. It is also observed through a statistical analysis that 72% of the solar wind speeds are between 415 km/s and 601 km/s during the two solar cycles during the corotating activity.

Figure 6 presents the distributions of solar wind (a) and (b) and the percentage distribution of solar wind speeds (c) and (d) in the magnetic cloud activity class during solar cycles 23 and 24. In this figure, we observe 42% and 32% of the speeds of the solar wind respectively during solar cycles 23 and 24, are greater than 450 km/s. Moreover the statistical analysis reveals that 71% of the solar velocities are between 354 km/s and 514 km/s during the two solar cycles during the magnetic cloud activity.

Figure 7 presents the solar wind distributions (a) and (b) and the percentage distribution of solar wind speeds (c) and (d) in the fluctuating activity class during solar cycles 23 and 24. This figure shows that 56% and 54% of the solar wind

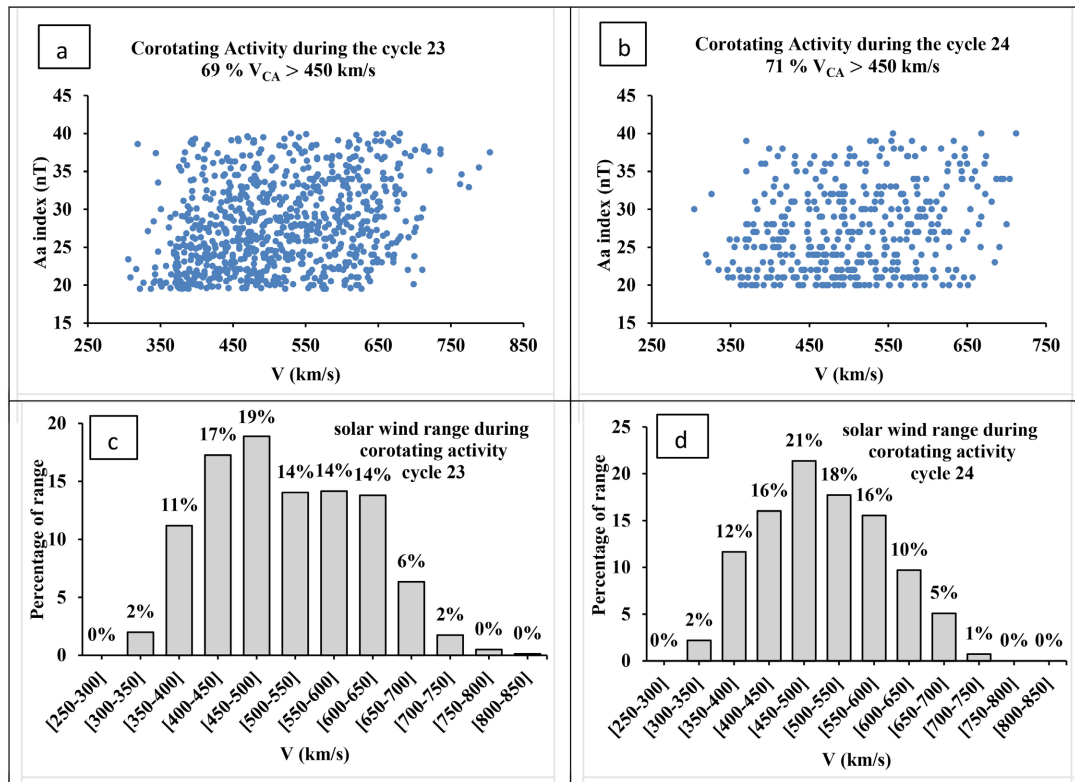


Figure 5. Solar wind distribution (a) and (b) and percentage distribution of solar wind speeds (c) and (d) in the corotating activity class during solar cycles 23 and 24.

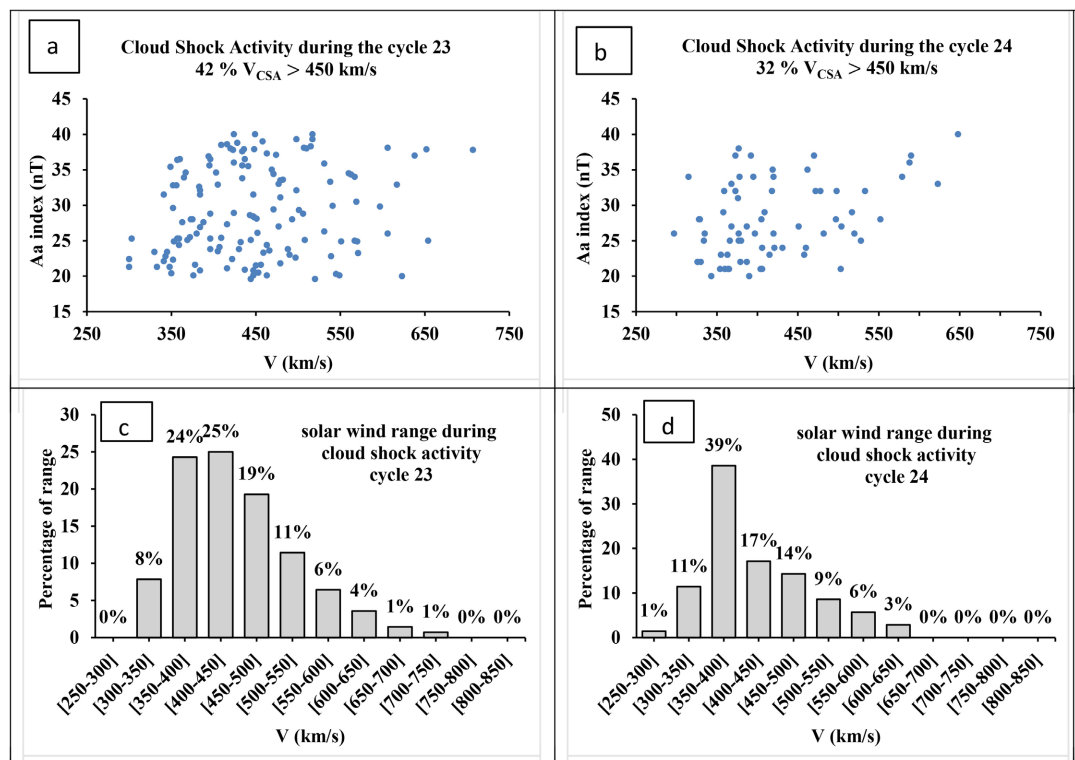


Figure 6. Solar wind distribution (a) and (b) and percentage distribution of solar wind speeds (c) and (d) in the magnetic cloud activity class during solar cycles 23 and 24.

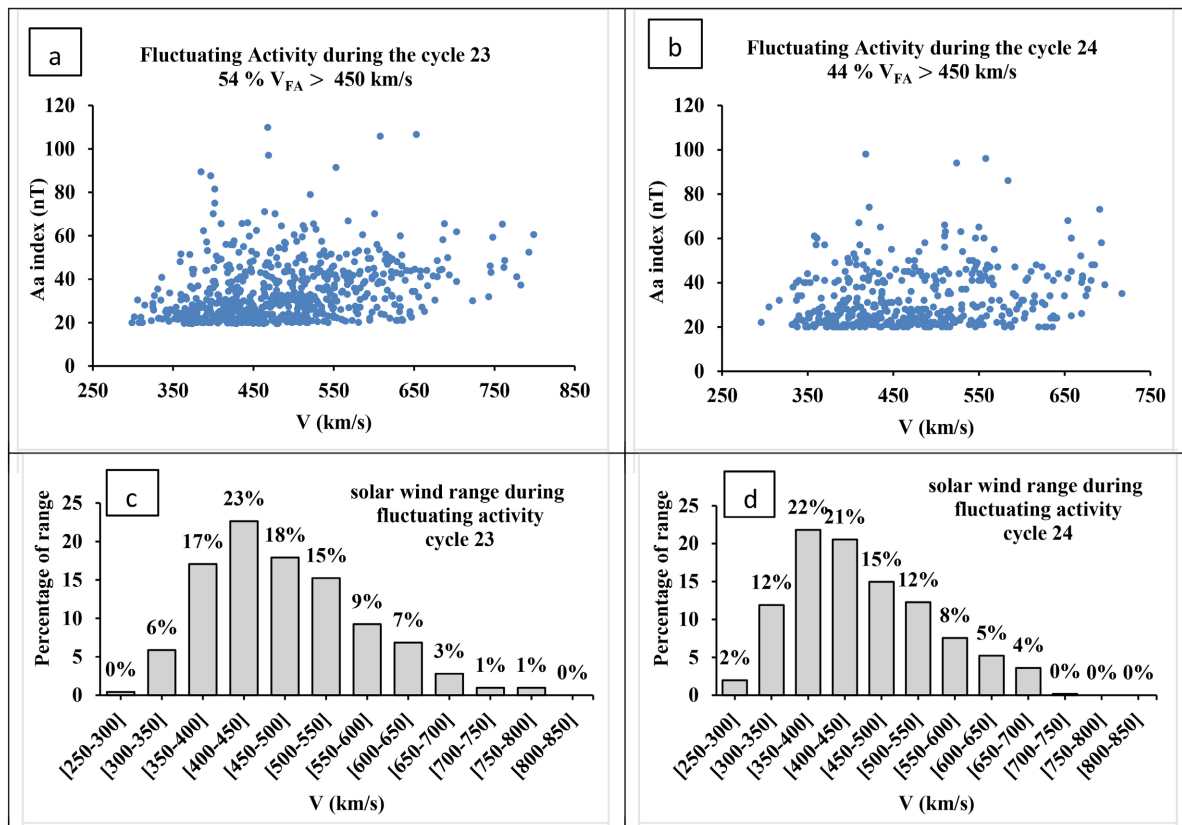


Figure 7. Solar wind distribution (a) and (b) and percentage distribution of solar wind speeds (c) and (d) in the fluctuating activity class during solar cycles 23 and 24.

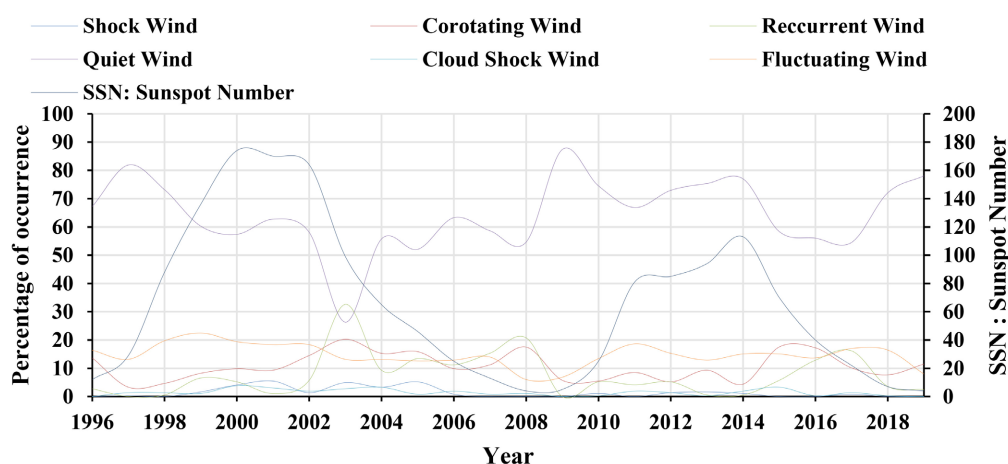
speeds respectively during solar cycles 23 and 24 are greater than 450 km/s. We also observe after a statistical analysis that 67% of the speeds of the solar wind are of the order of 478 ± 92 during the two solar cycles during the fluctuating activity.

In summary, our study shows that nearly 80% of the wind speeds $V < 450$ km/s are observed in the magnetic calm activity class. 88% of wind speeds $V > 450$ km/s, are observed in the recurrent activity class. 82% of the wind speeds $V > 450$ km/s, are observed in the shock activity class. About 70% of the wind speeds $V > 450$ km/s, are observed in the corotating activity class. The magnetic cloud and fluctuating activity classes show 37% and 55% of the solar wind speeds $V > 450$ km/s respectively. These observations confirm and extend the work of [2]. **Table 1** summarizes the order of magnitude of wind speeds by activity class.

Figure 8 presents the temporal evolution curves of the percentages of occurrences of the different classes of activity and the sunspot number during the period 1996 to 2019. This figure shows that each class of the solar wind is observed over the entire study period with different levels of occurrence. The highest percentages of slow solar wind are observed respectively in 1997 (87.12%) during solar cycle 23 and 2009 (88.76); 2014 (81.09%) and 2019 (80.82%) during solar cycle 24. The lowest percentages of slow wind occurrence are observed in 2003 (26.3%) during solar cycle 23 and 2017 (54.52%) during solar cycle 24. Shock

Table 1. Order of magnitude of solar wind speeds by activity class.

	Solar wind conditions
Quiet Activity	323 km/s à 459 km/s
Recurrent Activity	475 km/s à 675 km/s
Shock Activity	438km/s à 658 km/s
Corotating Activity	415 km/s à 601 km/s
Cloud Shock Activity	354 km/s à 514 km/s
Fluctuating Activity	386 km/s à 570 km/s

**Figure 8.** Curves of temporal evolution of the percentages of occurrences of the different classes of activity and the sunspot number during the period 1996 to 2019.

winds with a high level of occurrence are observed in 2000 (4.09%), 2001 (5.48%), 2003 (4.93%) and 2005 (5.2%) during the solar cycle 23 and 2012 (1.36%) and 2013 (1.64%) during solar cycle 24. The lowest percentages of shocks winds occurrence are observed respectively in 1996, 2007, 2008, 2009, 2011, 2015, 2016, 2018 and 2019 during the two solar cycle with an occurrence rate of 0%. The percentages of recurrent wind occurrence are observed in 2003 (32.6%) and exceptionally in 2008 (20.76%) during solar cycle 23 and in 2016 (12.84%) and 2017 (16.16%) during solar cycle 24. Low levels of recurrent wind occurrence are observed in 1997 and 2009 during both cycles with an occurrence rate of 0%. As for the corotating winds, the highest percentages of occurrence are observed in 2003 (20.27%), 2008 (17.48%), 2015 (17.53%), and in 2016 (17.21%) and the lowest percentages of occurrence in 1997 (3.28%) and in 2014 (4.38%) during the two solar cycles. The highest occurrence percentages of magnetic clouds are observed in 2000 (3.82%), 2001 (3.01%), 2004 (3.27%) and 2015 (3.28%) and the lowest percentages in 1996, 2009 and 2019 with an occurrence rate of 0%, during the two solar cycles. We observe a fairly similar level of fluctuation during our study period, but however, the fluctuation is quite significant around the solar maximum than at the solar minimum. These statistics show us that, slow winds are mainly observed at the minimum phase of each so-

lar cycle; but exceptionally the solar maximum of solar cycle 24, records a significant rate of slow wind. Shock winds are mostly observed around the solar maximum and recurrent winds are mostly observed at the descending phase of the solar cycle respectively. According to the work of [2] [4] [5] [19] [20] [21], the highest values of solar wind speed in Earth's orbit are observed during the descending phase of the solar cycle, when the high-speed fluxes from the equatorward extensions of the coronal holes polar extend to low heliographic latitudes. Corotating stable winds and moderate shock winds are mainly observed respectively at the descending phase and at the maximum phase.

Figure 9 presents the histograms of the percentages of occurrence of the different classes of solar activity according to the different phases of the solar cycle 23. In this figure, the slow solar wind flows mainly modulate the geomagnetism (77.53%) during the ascending phase of the solar cycle while the Earth experiences strong recurrent wind effects (18.43%) on the descending phase. Shock winds are mainly observed at the maximum phase of the solar cycle. The solar winds, stable in co-rotating and having moderate magnetic effects in the vicinity of the terrestrial environment, are important in the descending phase with 17.15%. As for the shock winds with a modification of the moderate level of activity, they were significant at the maximum and at the descending phase with respectively 2.46% and 2.26%. We observe a constant fluctuation of the wind on all the phases of the cycle. This leads to a permanent fluctuation of the heliosheet [5] [22].

Figure 10 presents the histograms of occurrences of the different classes of solar activity according to the different phases of the solar cycle 24. This figure shows that the slow winds are mainly observed at the minimum phase with 79.18% of the winds as well as at the maximum phase with 76.98% of the winds. The shock winds are mainly observed at the maximum phase with 1.1% of the winds. The solar winds, stable in co-rotation and having moderate magnetic effects in the vicinity of the terrestrial environment are important in the descending phase with 14.96% of the winds. Moderate shock winds are observed respectively

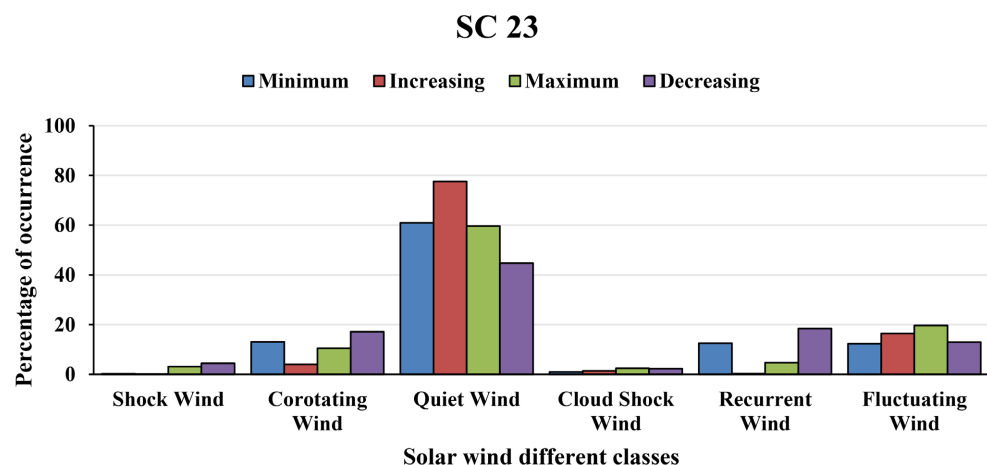


Figure 9. Histograms of the percentages of occurrences of the different classes of solar activity according to the different phases of the solar cycle 23.

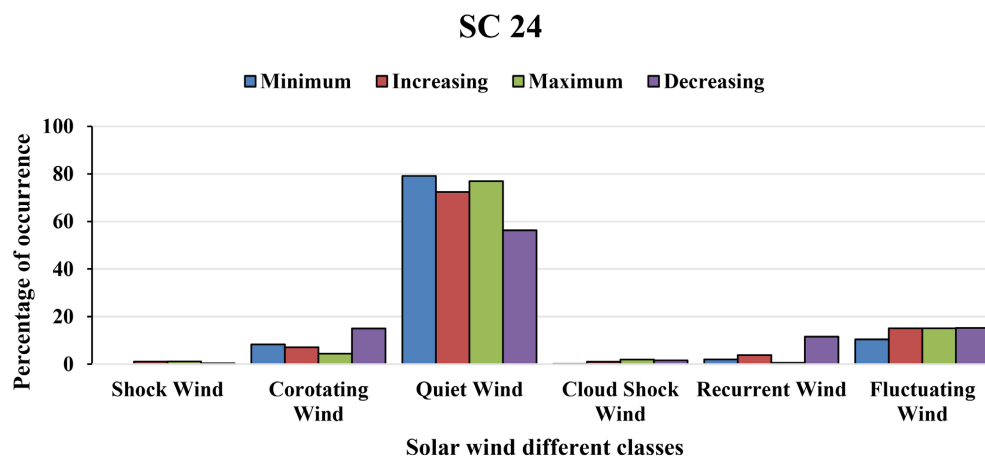


Figure 10. Histograms of the percentages of occurrences of the different classes of solar activity according to the different phases of the solar cycle 24.

at the maximum with 1.92% of the winds and at the descending phase of the cycle with 1.64% of the winds. A similar level of wind fluctuation is observed during the four phases of the solar cycle.

The analysis of **Figures 8-10** shows that the values of the speed of the solar wind during the solar cycle 23, is more important compared to the solar cycle 24. The solar cycle records a significant level of wind shock and recurrent compares at solar cycle 24. This is explained by the continued presence of so many low latitude holes so late in cycle 23, with recurrent high-velocity flows persisting in the ecliptic until early 2009, so is another consequence of weak polar fields [23]. High-velocity currents have the greatest relative effect on geomagnetic activity at high latitudes [2] [4] [5] [21] [24] [25] [26]. So we can say that the earth's atmosphere was much more disturbed during solar cycle 23 compared to solar cycle 24.

4. Conclusions

In this paper, we have analyzed the distribution of solar wind speeds according to the different classes of geomagnetic activity, using the classification of geomagnetic activity established by [2]. Our analysis shows that:

- Nearly 80% of the wind speeds $V < 450$ km/s are observed in the magnetic quiet activity class.
- 88% of wind speeds $V > 450$ km/s, are observed in the recurrent activity class.
- 82% of the wind speeds $V > 450$ km/s, are observed in the shock activity class.
- About 70% of the wind speeds $V > 450$ km/s, are observed in the corotating activity class.
- The magnetic cloud and fluctuating activity classes observed respectively 37% and 55% of the wind speeds $V > 450$ km/s.

We also analyzed the speed distribution of solar wind speeds according to the different classes of solar activity and the different phases of the solar cycle using

the classification established by [2]. We found that slow winds are observed mainly at minimum phase of each solar cycle; but exceptionally the solar maximum of solar cycle 24, records a significant rate of slow wind. Shock winds are mainly observed around the solar maximum and recurrent winds are mainly observed at the descending phase of the solar cycle respectively. Corotating stable winds and moderate shock winds dominate respectively at the descending phase and at the maximum phase.

Acknowledgements

The authors would like to thank the reviewers for their detailed and insightful comments and constructive suggestions. Special thanks to all providers of data used (OMNIweb from NASA Goddard Space Flight Center to provide solar wind data; Royal Observatory of Belgium for providing sunspot number). International Services of Geomagnetic Indices to provide Aa index.

Conflicts of Interest

The authors have not declared any conflicts of interests.

References

- [1] Owens, M.J., Lockwood, M. and Riley, P. (2017) Global Solar Wind Variations over the Last Four Centuries. *Scientific Reports*, **7**, Article No. 41548. <https://doi.org/10.1038/srep41548>
- [2] Zerbo, J.L., Amory-Mazaudier, C., Frédéric, O. and Richardson, J. (2012) Solar Wind and Geomagnetism: Toward a Standard Classification of Geomagnetic Activity from 1868 to 2009. *Annales Geophysicae*, **30**, 421-426. <https://doi.org/10.5194/angeo-30-421-2012>
- [3] Altschuler, M.D. and Newkirk, G. (1969) Magnetic Fields and the Structure of the Solar Corona. *Solar Physics*, **9**, 131-149. <https://doi.org/10.1007/BF00145734>
- [4] Legrand, J.-P. and Simon, P.A. (1989) Solar Cycle and Geomagnetic Activity: A Review for Geophysicists. Part 1. The Contributions to Geomagnetic Activity of Shock Waves and of the Solar Wind. *Annales Geophysicae*, **7**, 565-593.
- [5] Zerbo, J.L., Ouattara, F. and Nanema, E. (2015) On Solar Wind Speed Distribution and Geomagnetic Activity during Solar Cycle 23 and the Early Ascending Phase of Solar Cycle 24. *Iranian Journal of Pharmaceutical Sciences*, **10**, 562-567. <https://doi.org/10.5897/IJPS2015.4401>
- [6] Owens, M.J., Crooker, N.U. and Lockwood, M. (2014) Solar Cycle Evolution of Dipolar and Pseudostreamer Belts and Their Relation to the Slow Solar Wind. *Journal of Geophysical Research: Space Physics*, **119**, 36-46. <https://doi.org/10.1002/2013JA019412>
- [7] Owens, M. (2020) Solar-Wind Structure. Oxford Research Encyclopedia of Physics. Oxford University Press, Oxford. <https://doi.org/10.1093/acrefore/9780190871994.013.19>
- [8] Webb, D.F. and Howard, T.A. (2012) Coronal Mass Ejections: Observations. *Living Reviews in Solar Physics*, **9**, Article No. 3. <https://doi.org/10.12942/lrsp-2012-3>
- [9] Gosling, J.T. (1993) The Solar Flare Myth. *Journal of Geophysical Research: Space Physics*, **98**, 18937-18949. <https://doi.org/10.1029/93JA01896>

- [10] Richardson, I.G., Cane, H.V. and Cliver, E.W. (2002) Sources of Geomagnetic Activity during Nearly Three Solar Cycles (1972-2000). *Journal of Geophysical Research: Space Physics*, **107**, SSH 8-1-SSH 8-13. <https://doi.org/10.1029/2001JA000504>
- [11] Kilpua, E.K.J., Balogh, A., von Steiger, R. and Liu, Y.D. (2017) Geoeffective Properties of Solar Transients and Stream Interaction Regions. *Space Science Reviews*, **212**, 1271-1314. <https://doi.org/10.1007/s11214-017-0411-3>
- [12] Vršnak, B. and Gopalswamy, N. (2002) Influence of the Aerodynamic Drag on the Motion of Interplanetary Ejecta. *Journal of Geophysical Research: Space Physics*, **107**, SSH 2-1-SSH 2-6. <https://doi.org/10.1029/2001JA000120>
- [13] Cargill, P.J. (2004) On the Aerodynamic Drag Force Acting on Interplanetary Coronal Mass Ejections. *Solar Physics*, **221**, 135-149. <https://doi.org/10.1023/B:SOLA.0000033366.10725.a2>
- [14] Case, A., Spence, H., Owens, M., Riley, P. and Odstrcil, D. (2008) Ambient Solar Wind's Effect on ICME Transit Times. *Geophysical Research Letters*, **35**, L15105. <https://doi.org/10.1029/2008GL034493>
- [15] Luhmann, J.G., Ledvina, S.A., Odstrcil, D., Owens, M.J., Zhao, X.-P., Liu, Y. and Riley, P. (2010) Cone Model-Based SEP Event Calculations for Applications to Multipoint Observations. *Advances in Space Research*, **46**, 1-21. <https://doi.org/10.1016/j.asr.2010.03.011>
- [16] Chollet, E.E. and Giacalone, J. (2011) Evidence of Confinement of Solar-Energetic Particles to Interplanetary Magnetic Field Lines. *Astrophysical Journal*, **728**, Article No. 64. <https://doi.org/10.1088/0004-637X/728/1/64>
- [17] Ouattara, F. and Amory-Mazaudier, C. (2009) Solar-Geomagnetic Activity and Aa Indices toward a Standard Classification. *Journal of Atmospheric and Solar-Terrestrial Physics*, **71**, 1736-1748. <https://doi.org/10.1016/j.jastp.2008.05.001>
- [18] Svalgaard, L. (1977) Geomagnetic Activity: Dependence on Solar Wind Parameters. University of California Institute for Plasma Research, Stanford.
- [19] Krieger, A.S., Timothy, A.F. and Roelof, E.C. (1973) A Coronal Hole and Its Identification as the Source of a High Velocity Solar Wind Stream. *Solar Physics*, **29**, 505-525. <https://doi.org/10.1007/BF00150828>
- [20] Gosling, J.T., Asbridge, J.R., Bame, S.J. and Feldman, W.C. (1976) Solar Wind Speed Variations: 1962-1974. *Journal of Geophysical Research* (1896-1977), **81**, 5061-5070. <https://doi.org/10.1029/JA081i028p05061>
- [21] Richardson, I.G. and Cane, H.V. (2012) Solar Wind Drivers of Geomagnetic Storms during More than Four Solar Cycles. *Journal of Space Weather and Space Climate*, **2**, A01. <https://doi.org/10.1051/swsc/2012001>
- [22] Simon, P.A. and Legrand, J.P. (1987) Some Solar Cycle Phenomena Related to the Geomagnetic Activity from 1868 to 1980 III. Quiet-Days, Fluctuating Activity or the Solar Equatorial Belt as the Main Origin of the Solar Wind Flowing in the Ecliptic Plane. *Astronomy & Astrophysics*, **182**, 329.
- [23] Wang, Y.-M., Robbrecht, E. and Sheeley, N.R. (2009) On the Weakening of the Polar Magnetic Fields during Solar Cycle 23. *ApJ*, **707**, 1372-1386. <https://doi.org/10.1088/0004-637X/707/2/1372>
- [24] Finch, I.D., Lockwood, M.L. and Rouillard, A.P. (2008) Effects of Solar Wind Magnetosphere Coupling Recorded at Different Geomagnetic Latitudes: Separation of Directly-Driven and Storage/Release Systems. *Geophysical Research Letters*, **35**, L21105. <https://doi.org/10.1029/2008GL035399>
- [25] Lukianova, R., Mursula, K. and Kozlovsky, A. (2012) Response of the Polar Mag-

- netic Field Intensity to the Exceptionally High Solar Wind Streams in 2003. *Geophysical Research Letters*, **39**, L04101. <https://doi.org/10.1029/2011GL050420>
- [26] Holappa, L., Mursula, K., Asikainen, T. and Richardson, I.G. (2014) Annual Fractions of High-Speed Streams from Principal Component Analysis of Local Geomagnetic Activity. *Journal of Geophysical Research: Space Physics*, **119**, 4544-4555. <https://doi.org/10.1002/2014JA019958>